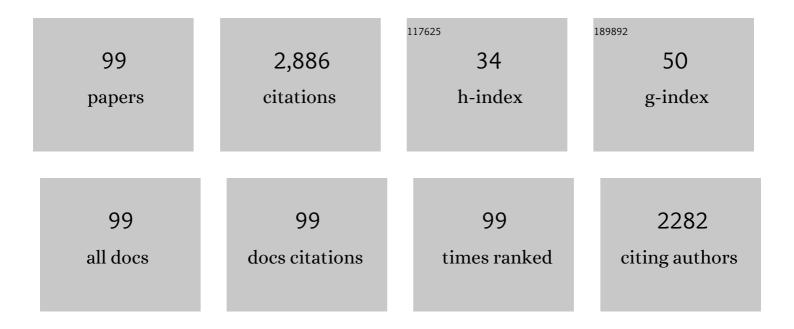
List of Publications by Year in descending order

Source: https://exaly.com/author-pdf/1761300/publications.pdf Version: 2024-02-01



HUIVII CHEN

#	Article	IF	CITATIONS
1	The CuCo2O4/CuO composite-based microspheres serve as a battery-type cathode material for highly capable hybrid supercapacitors. Journal of Alloys and Compounds, 2022, 894, 162566.	5.5	19
2	Battery-type and binder-free MgCo2O4-NWs@NF electrode materials for the assembly of advanced hybrid supercapacitors. International Journal of Hydrogen Energy, 2022, 47, 15807-15819.	7.1	56
3	Electrospun NiO/C nanofibers as electrode materials for hybrid supercapacitors with superior electrochemical performance. International Journal of Hydrogen Energy, 2022, 47, 16985-16995.	7.1	21
4	Facile growth of nickel foam-supported MnCo2O4.5 porous nanowires as binder-free electrodes for high-performance hybrid supercapacitors. Journal of Energy Storage, 2022, 50, 104297.	8.1	70
5	Growth of uniform CuCo2O4 porous nanosheets and nanowires for high-performance hybrid supercapacitors. Journal of Energy Storage, 2022, 52, 105048.	8.1	64
6	Porous MgCo2O4 nanoflakes serve as electrode materials for hybrid supercapacitors with excellent performance. Journal of Colloid and Interface Science, 2022, 625, 925-935.	9.4	99
7	A review on the synthesis of CuCo2O4-based electrode materials and their applications in supercapacitors. Journal of Materiomics, 2021, 7, 98-126.	5.7	115
8	Template-free synthesis of novel Co3O4 micro-bundles assembled with flakes for high-performance hybrid supercapacitors. Ceramics International, 2021, 47, 716-724.	4.8	34
9	Simple synthesis of honeysuckle-like CuCo2O4/CuO composites as a battery type electrode material for high-performance hybrid supercapacitors. International Journal of Hydrogen Energy, 2021, 46, 66-79.	7.1	52
10	MgCo ₂ O ₄ -based electrode materials for electrochemical energy storage and conversion: a comprehensive review. Sustainable Energy and Fuels, 2021, 5, 4807-4829.	4.9	94
11	Uniform MnCo ₂ O _{4.5} porous nanowires and quasi-cubes for hybrid supercapacitors with excellent electrochemical performances. Nanoscale Advances, 2021, 3, 4447-4458.	4.6	41
12	Porous CuCo2O4 microtubes as a promising battery-type electrode material for high-performance hybrid supercapacitors. Journal of Materiomics, 2021, 7, 1358-1368.	5.7	59
13	Battery-type CuCo2O4/CuO nanocomposites as positive electrode materials for highly capable hybrid supercapacitors. Ceramics International, 2021, 47, 24877-24886.	4.8	32
14	High-performance hybrid supercapacitor based on the porous copper cobaltite/cupric oxide nanosheets as a battery-type positive electrode material. International Journal of Hydrogen Energy, 2021, 46, 28144-28155.	7.1	32
15	Uniform MgCo2O4 porous nanoflakes and nanowires with superior electrochemical performance for asymmetric supercapacitors. Journal of Alloys and Compounds, 2021, 884, 161087.	5.5	32
16	Facile solvothermal synthesis of novel MgCo2O4 twinned-hemispheres for high performance asymmetric supercapacitors. Journal of Alloys and Compounds, 2020, 818, 152905.	5.5	68
17	Hydrothermal synthesis of Fe-doped Co3O4 urchin-like microstructures with superior electrochemical performances. Journal of Alloys and Compounds, 2020, 821, 153507.	5.5	38
18	Solvothermal synthesis of novel pod-like MnCo2O4.5 microstructures as high-performance electrode materials for supercapacitors. International Journal of Hydrogen Energy, 2020, 45, 3016-3027.	7.1	50

#	Article	IF	CITATIONS
19	Bundlelike CuCo ₂ O ₄ Microstructures Assembled with Ultrathin Nanosheets As Battery-Type Electrode Materials for High-Performance Hybrid Supercapacitors. ACS Applied Energy Materials, 2020, 3, 8026-8037.	5.1	172
20	Simple Preparation of Porous FeCo ₂ O ₄ Microspheres and Nanosheets for Advanced Asymmetric Supercapacitors. ACS Applied Energy Materials, 2020, 3, 11307-11317.	5.1	52
21	Simple preparation of ZnCo2O4 porous quasi-cubes for high performance asymmetric supercapacitors. Applied Surface Science, 2020, 515, 146008.	6.1	51
22	Facile hydrothermal synthesis of porous MgCo ₂ O ₄ nanoflakes as an electrode material for high-performance asymmetric supercapacitors. Nanoscale Advances, 2020, 2, 3263-3275.	4.6	41
23	Hydrothermal synthesis of flower-like MgCo2O4 porous microstructures as high-performance electrode material for asymmetric supercapacitors. Journal of Alloys and Compounds, 2020, 824, 153939.	5.5	53
24	Highly aligned magnetic composite nanofibers fabricated by magnetic-field-assisted electrospinning PAN/FeCo solution. High Performance Polymers, 2019, 31, 230-237.	1.8	10
25	Facile synthesis of mesoporous ZnCo2O4 hierarchical microspheres and their excellent supercapacitor performance. Ceramics International, 2019, 45, 8577-8584.	4.8	72
26	Facile synthesis of porous Mn-doped Co3O4 oblique prisms as an electrode material with remarkable pseudocapacitance. Ceramics International, 2019, 45, 8008-8016.	4.8	51
27	Rapid hydrothermal synthesis of snowflake-like ZnCo2O4/ZnO mesoporous microstructures with excellent electrochemical performances. Ceramics International, 2019, 45, 12243-12250.	4.8	49
28	Simple solvothermal synthesis of magnesium cobaltite microflowers as a battery grade material with high electrochemical performances. Ceramics International, 2019, 45, 14642-14651.	4.8	41
29	Uniform and porous Mn-doped Co3O4 microspheres: Solvothermal synthesis and their superior supercapacitor performances. Ceramics International, 2019, 45, 11876-11882.	4.8	60
30	Intrinsically stretchable conductors and interconnects for electronic applications. Materials Chemistry Frontiers, 2019, 3, 1032-1051.	5.9	21
31	Egg Albumin-Assisted Hydrothermal Synthesis of Co3O4 Quasi-Cubes as Superior Electrode Material for Supercapacitors with Excellent Performances. Nanoscale Research Letters, 2019, 14, 340.	5.7	29
32	Solvothermal preparation of zinc cobaltite mesoporous microspheres for high-performance electrochemical supercapacitors. Journal of Alloys and Compounds, 2019, 781, 425-432.	5.5	34
33	Hydrothermal synthesis of mesoporous MnCo2O4/CoCo2O4 ellipsoid-like microstructures for high-performance electrochemical supercapacitors. Ceramics International, 2019, 45, 7244-7252.	4.8	47
34	Simple growth of mesoporous zinc cobaltite urchin-like microstructures towards high-performance electrochemical capacitors. Ceramics International, 2019, 45, 4059-4066.	4.8	38
35	MnO2 hierarchical microspheres assembled from porous nanoplates for high-performance supercapacitors. Ceramics International, 2019, 45, 1058-1066.	4.8	69
36	Hydrothermal synthesis of novel Ni microflowers with enhanced ferromagnetic properties. Micro and Nano Letters, 2019, 14, 455-457.	1.3	3

#	Article	IF	CITATIONS
37	Templateâ€free synthesis of novel urchinâ€like nickel microstructures with enhanced ferromagnetic properties. Micro and Nano Letters, 2019, 14, 812-814.	1.3	0
38	Formation of Ni microflowers constructed by solid-particle-core and petal-shell with increased coercivity. Materials Letters, 2018, 217, 223-226.	2.6	0
39	CTAB-assisted synthesis of eight-horn-shaped Cu2O crystals via a simple solution approach. Journal of Materials Science: Materials in Electronics, 2018, 29, 4256-4260.	2.2	2
40	Template-free hydrothermal synthesis of 3D hierarchical Co3O4 microflowers constructed by mesoporous nanoneedles. Materials Letters, 2018, 215, 179-182.	2.6	12
41	CTAB-assisted hydrothermal synthesis of Cu2Se films composed of nanowire networks. Materials Letters, 2018, 210, 62-65.	2.6	16
42	Dendrite-like cupric oxide microstructures prepared via a facile SDBS-assisted hydrothermal route. Journal of Materials Science: Materials in Electronics, 2018, 29, 3178-3181.	2.2	2
43	Large scale synthesis of ultrathin cupric oxide nanosheets via a rapid microwave-assisted and template-free route. Materials Letters, 2018, 214, 138-141.	2.6	2
44	Solvothermal synthesis of porous MnCo2O4.5 spindle-like microstructures as high-performance electrode materials for supercapacitors. Ceramics International, 2018, 44, 22622-22631.	4.8	57
45	Rapid and template-free synthesis of Cu2O truncated octahedra using glucose as green reducing agent. Materials Letters, 2018, 210, 31-34.	2.6	21
46	Glass fabric@cobalt core-shell composites: Electroless plating fabrication and their enhanced magnetic properties. Materials Letters, 2017, 188, 80-83.	2.6	5
47	Hydrothermal synthesis of flower-like zinc oxide microstructures with large specific surface area. Journal of Materials Science: Materials in Electronics, 2017, 28, 16855-16860.	2.2	9
48	Simple synthesis of novel mushroom-like FeNi3 microstructures by a hydrothermal reduction. Materials Research Innovations, 2017, , 1-4.	2.3	1
49	Electroless deposition of pure copper film on carbon fabric substrate using hydrazine as reducing agent. Journal of Materials Science: Materials in Electronics, 2017, 28, 13869-13872.	2.2	4
50	Fabrication of copper-coated glass fabric composites through electroless plating process. Journal of Materials Science: Materials in Electronics, 2017, 28, 798-802.	2.2	11
51	Silver-coated glass fabric composites prepared by electroless plating. Materials Letters, 2016, 180, 144-147.	2.6	25
52	Novel chain-like cobalt–nickel microstructures fabricated by a CTAB-assisted hydrothermal method. Materials Letters, 2016, 166, 188-191.	2.6	6
53	Large-scale synthesis of highly porous carbon nanosheets for supercapacitor electrodes. Journal of Alloys and Compounds, 2016, 677, 105-111.	5.5	68
54	Facile synthesis of highly porous N-doped CNTs/Fe ₃ C and its electrochemical properties. RSC Advances, 2016, 6, 44013-44018.	3.6	13

#	Article	IF	CITATIONS
55	Bamboo chopsticks-derived porous carbon microtubes/flakes composites for supercapacitor electrodes. Materials Letters, 2016, 185, 359-362.	2.6	21
56	Conductive nickel/carbon fiber composites prepared via an electroless plating route. Journal of Materials Science: Materials in Electronics, 2016, 27, 5686-5690.	2.2	11
57	Copper@carbon fiber composites prepared by a simple electroless plating technique. Materials Letters, 2016, 173, 211-213.	2.6	23
58	Conductive glass fabrics@nickel composites prepared by a facile electroless deposition method. Materials Letters, 2016, 171, 158-161.	2.6	16
59	Surfactant-assisted hydrothermal synthesis of 3D urchin-like cobalt–nickel microstructures. Materials Letters, 2016, 162, 13-16.	2.6	6
60	Facile and green synthesis of mesoporous Co 3 O 4 nanowires. Materials Letters, 2016, 163, 72-75.	2.6	21
61	Facile synthesis of ellipsoidal hematite nanostructures via an EDA-assisted solvothermal method. Journal of Materials Science: Materials in Electronics, 2015, 26, 5446-5450.	2.2	3
62	A general route to the synthesis of PS/metal composites and their conversion to metal hollow microspheres. Journal of Materials Science: Materials in Electronics, 2015, 26, 10049-10054.	2.2	1
63	Facile synthesis of electromagnetic Ni@glass fiber composites via electroless deposition method. Journal of Materials Science: Materials in Electronics, 2015, 26, 3530-3537.	2.2	7
64	PVP-assisted synthesis of flower-like hematite microstructures composed of porous nanosheets. Journal of Materials Science: Materials in Electronics, 2015, 26, 2982-2986.	2.2	3
65	Rapid and simple synthesis of 3D ZnO microflowers at room temperature. Materials Letters, 2015, 158, 347-350.	2.6	6
66	Porous hematite microflowers toward the adsorption of organic pollutants from water. Materials Letters, 2015, 159, 64-67.	2.6	5
67	Electroless deposition method for silverâ€coated carbon fibres. Micro and Nano Letters, 2015, 10, 315-317.	1.3	13
68	Solvothermal synthesis of cauliflower-like CoNi microstructures with enhanced magnetic property. Materials Letters, 2015, 142, 246-249.	2.6	5
69	Template-free synthesis of magnetic CoNi nanoparticles via a solvothermal method. Materials Letters, 2015, 138, 158-161.	2.6	15
70	Hydrothermal synthesis of chainâ€ŀike nickel microstructures with enhanced magnetic properties. Micro and Nano Letters, 2014, 9, 261-263.	1.3	3
71	Electroless plating route to the synthesis of glass microspheres/copper composites with excellent conductivity. Micro and Nano Letters, 2014, 9, 770-774.	1.3	3
72	Silver-coated glass fibers prepared by a simple electroless plating technique. Journal of Materials Science: Materials in Electronics, 2014, 25, 4638-4642.	2.2	35

Ηυιγυ Chen

#	Article	IF	CITATIONS
73	Facile and controlled synthesis of FeCo nanoparticles via a hydrothermal method. Journal of Materials Science: Materials in Electronics, 2014, 25, 1965-1969.	2.2	7
74	Chain-like CoNi alloy microstructures fabricated by a PVP-assisted solvothermal process. Materials Letters, 2014, 131, 306-309.	2.6	18
75	Large-scale synthesis of ultralong copper nanowires via a facile ethylenediamine-mediated process. Journal of Materials Science: Materials in Electronics, 2014, 25, 2344-2347.	2.2	5
76	Fabrication of conductive copper-coated glass fibers through electroless plating process. Journal of Materials Science: Materials in Electronics, 2014, 25, 2611-2617.	2.2	33
77	Preparation of hierarchical cobalt dendritic flowers via a simple solvothermal approach. Journal of Materials Science: Materials in Electronics, 2014, 25, 3448-3454.	2.2	1
78	Hydrothermal synthesis of β-Ni(OH)2 platelets and their thermal conversion to NiO. Journal of Materials Science: Materials in Electronics, 2014, 25, 3716-3720.	2.2	6
79	Hydrothermal synthesis of silver crystals via a sodium chloride assisted route. Materials Letters, 2014, 136, 175-178.	2.6	7
80	Fabrication of cobalt hollow microspheres via a PVP-assisted solvothermal process. Materials Letters, 2013, 110, 87-90.	2.6	13
81	Solvothermal synthesis and characterization of copper indium diselenide microflowers. Materials Letters, 2013, 106, 79-82.	2.6	7
82	Conductive and magnetic glass microsphere/cobalt composites prepared via an electroless plating route. Materials Letters, 2013, 112, 97-100.	2.6	12
83	Cobalt microtrees assembled by dendrites: Hydrothermal synthesis and their enhanced magnetic properties. Materials Letters, 2013, 99, 1-4.	2.6	9
84	Low-temperature solution synthesis of CuO nanorods with thin diameter. Materials Letters, 2013, 93, 60-63.	2.6	47
85	Preparation and magnetic property of chain-like cobalt microrods. Materials Research Bulletin, 2013, 48, 2399-2402.	5.2	8
86	Template-free formation of urchin-like FeNi3 microstructures by hydrothermal reduction. Materials Letters, 2013, 91, 75-77.	2.6	10
87	Formation of flower-like magnesium hydroxide microstructure via a solvothermal process. Electronic Materials Letters, 2012, 8, 529-533.	2.2	14
88	Synthesis and characterization of CuInSe2 nanoparticles via a solution method. Materials Research Bulletin, 2012, 47, 2730-2734.	5.2	7
89	Template-free synthesis and characterization of dendritic cobalt microstructures by hydrazine reduction route. Materials Research Bulletin, 2012, 47, 4353-4358.	5.2	17
90	Flower-like hierarchical nickel microstructures: Facile synthesis, growth mechanism, and their magnetic properties. Materials Research Bulletin, 2012, 47, 1839-1844.	5.2	38

Ηυιγυ Chen

#	Article	IF	CITATIONS
91	Controlled synthesis and characterisation of flower-like cobalt microstructures. Micro and Nano Letters, 2011, 6, 122.	1.3	5
92	Green synthesis and characterization of se nanoparticles and nanorods. Electronic Materials Letters, 2011, 7, 333-336.	2.2	46
93	Synthesis and characterization of hollow silver spheres at room temperature. Electronic Materials Letters, 2011, 7, 151-154.	2.2	15
94	Metallic Copper Nanostructures Synthesized by a Facile Hydrothermal Method. Journal of Nanoscience and Nanotechnology, 2010, 10, 629-636.	0.9	47
95	Solvothermal Synthesis and Characterization of Chalcopyrite CuInSe2 Nanoparticles. Nanoscale Research Letters, 2010, 5, 217-223.	5.7	102
96	Selenium nanowires and nanotubes synthesized via a facile template-free solution method. Materials Research Bulletin, 2010, 45, 699-704.	5.2	78
97	Three-Dimensional CuO Nanobundles Consisted of Nanorods: Hydrothermal Synthesis, Characterization, and Formation Mechanism. Journal of Nanoscience and Nanotechnology, 2010, 10, 5121-5128.	0.9	14
98	Synthesis of chalcopyrite CuInSe <inf>2</inf> nanoparticles via a facile solvothermal method. , 2010, , .		0
99	Synthesis and characterization of CuSe and InSe nanoparticles for CuInSe <inf>2</inf> based solar cell application. , 2009, , .		0